

**BIOCHEMICAL CHARACTERISATION OF
DYSTROPHIN IN SENSORY DENDRITE AND
EPITHELIAL CELLS OF
*DROSOPHILA MELANOGASTER***

TEE CHEE WEI

UNIVERSITI SAINS MALAYSIA

2020

**BIOCHEMICAL CHARACTERISATION OF
DYSTROPHIN IN SENSORY DENDRITE AND
EPITHELIAL CELLS OF
*DROSOPHILA MELANOGASTER***

by

TEE CHEE WEI

Thesis submitted in fulfilment of the requirements

for the degree of

Doctor of Philosophy

January 2020

ACKNOWLEDGEMENT

The scientific work presented in this thesis was performed in close collaboration between Universiti Sains Malaysia and Rikagaku Kenkyūjyo or RIKEN in Wako-shi, Saitama-ken, Japan under 3 years program for junior scientists, i.e. International Program Associate (IPA).

First and foremost, I felt very fortunate and appreciated to be given a chance to conduct my experiments in one of the world renowned institutes, RIKEN Brain Science Institute. This truly enlightened me on how people carried out the fundamental research in neuroscience. More important, it provided me with opportunity to learn and interact with various researchers from different fields and countries. This indirectly changed my perspective about ins and outs of science and gave an idea of future career to be.

The personal financial assistance and the postgraduate study fee sponsored by Kementerian Pendidikan Tinggi Malaysia under MyBrain15 MyPhD scheme were deeply appreciated. Besides, RIKEN also generously provided sufficient allowance and housing to cover a costly daily living expense and insurance coverage for accidents as well.

This work was supervised by main supervisor, Professor Shaharum Shamsuddin at Pusat Pengajian Sains Kesihatan, Universiti Sains Malaysia, Kelantan and co-supervisor, Dr. Mohd. Ghows Mohd. Azzam at Pusat Pengajian Sains Kajihayat, Universiti Sains Malaysia, Pulau Pinang. Therefore, I would like to express my sincere gratitude for their advice and undeniable support, especially for Prof. Shaharum Shamsuddin. Their visiting to Japan and treating made me feel the warmest regards far from hometown. Special thanks go to Dr. Adrian Walton Moore,

team leader of the laboratory for Genetic Control of Neuronal Architecture, and Dr. Marc Anthony Macchi, research scientist at RIKEN Brain Science Institute for their proper guidance and helpful advice. Another special guests that I would like to thank are Prof. Sudesh Kumar at School of Biological Science, Universiti Sains Malaysia for his prudent advice and guidance and Dr. Yoong Li Foong, research scientist at RIKEN Brain Science Institute for her comments and feedback on this thesis. In addition, I would like to thank RIKEN BSI-Olympus Collaboration Center (BOCC) and RIKEN BSI Research Resources Center (RRC) for providing their excellent laboratory services.

Meanwhile, I would like to thank Malaysian and Japanese colleagues that offering their helping hands in, ranged from daily life to research in academia. Undeniably without them, geographical barrier, language and culture differences posed me the biggest uneasy challenges along my study. Here, I wish the friendship bonded hitherto would be lasted as longer as possible.

Last but not least, I would like to thank my family for their greatest spiritual supports and helping in document works along my study in Japan.

TABLE OF CONTENTS

ACKNOWLEDGEMENT	ii
TABLE OF CONTENTS	iv
LIST OF TABLES	x
LIST OF FIGURES	xii
LIST OF SYMBOLS	xvii
LIST OF ABBREVIATIONS	xviii
ABSTRAK	xx
ABSTRACT	xxii
CHAPTER 1 INTRODUCTION	1
1.1 Background of study	1
1.2 Statement of problem	3
1.3 Hypothesis	3
1.4 Rationale of study.....	3
1.5 General and specific objectives	5
1.5.1 General objectives.....	5
1.5.2 Specific objectives	5
CHAPTER 2 LITERATURE REVIEW	6
2.1 <i>Drosophila melanogaster</i>	6
2.1.1 Introduction.....	6
2.1.2 <i>Drosophila</i> life cycles	6
2.1.3 GAL4-UAS system in <i>Drosophila</i>	8
2.1.4 Balancer chromosomes	9
2.2 Neurons and dendrites	11
2.3 <i>Drosophila</i> dendrites	14
2.4 Transcriptional control of dendritic morphology	16

2.5	The larval body wall.....	18
2.6	Dystrophin: An important component of cell membrane.....	22
2.7	Transcription of <i>dystrophin</i> gene in human	22
2.8	Transcription of <i>dystrophin</i> gene in <i>Drosophila</i>	25
2.9	Dystrophin protein structure.....	27
2.10	Dystrophin and its protein homologue in integrity of musculature	29
2.11	Dystrophin in neurons	33
2.12	Gene therapy, mini- and micro- <i>dystrophin</i>	35
2.13	Dystroglycan	37
2.14	Adenomatous Polyposis Coli	37
2.15	The Target of Rapamycin.....	38
2.16	Microtubules.....	39
CHAPTER 3 MATERIALS AND METHODS		40
3.1	Experimental design.....	40
3.2	Materials.....	44
3.2.1	Chemicals and reagents.....	44
3.2.2	Enzymes and antibodies.....	44
3.2.3	Kits	44
3.2.4	Consumables	44
3.2.5	General instruments	44
3.2.6	DNA materials and vectors	52
3.2.7	Bacterial strains.....	52
3.2.8	Fly stocks	52
3.3	Microbiological methods.....	61
3.3.1	Media and solutions	61
3.3.1(a)	Luria Bertani (LB) broth.....	61
3.3.1(b)	Luria Bertani (LB) agar-plates	61

3.3.2	Autoclave sterilization	61
3.3.3	<i>Escherichia coli</i> (<i>E. coli</i>) strains used in this study	62
3.3.4	Long-term storage of <i>E. coli</i>	62
3.3.5	Preparation of antibiotics	62
3.4	Recombinant DNA methods	62
3.4.1	Preparation of oligonucleotides	62
3.4.2	Purification of the plasmid DNA	64
3.4.2(a)	Plasmid mini prep	64
3.4.2(b)	Plasmid midi prep	65
3.4.3	DNA plasmid digestion	66
3.4.4	1% (w/v) agarose gel for DNA gel electrophoresis	66
3.4.5	DNA gel electrophoresis	66
3.4.6	Polymerase Chain Reaction (PCR)	67
3.4.7	Purification of PCR product using kit	67
3.4.8	DNA gel extraction	69
3.4.9	<i>Escherichia coli</i> competent cell preparation	70
3.4.10	Cloning of PCR product into pCR TM -Blunt II-TOPO TM vector	70
3.4.11	Transformation of plasmids into chemically competent <i>E. coli</i>	70
3.4.12	Directional cloning into plasmid vector	72
3.5	Protein techniques and analyses	72
3.5.1	Protein expression and purification	72
3.5.2	Buffer exchange by dialysis	74
3.5.3	Protein concentration measurement	74
3.5.4	Sodium dodecyl sulphate-polyacrylamide gel electrophoresis (SDS-PAGE)	75
3.5.5	Coomassie brilliant blue staining	78
3.5.6	Western blotting	78
3.5.7	Western blot hybridization	79

3.6	<i>Drosophila</i> techniques.....	79
3.6.1	Fly husbandry.....	79
3.6.2	Collecting <i>Drosophila</i> virgin females.....	82
3.6.3	<i>Drosophila</i> embryo injection protocol.....	82
3.6.4	Transgenic RNAi knockdown in <i>Drosophila</i>	82
3.6.5	PCR genotyping protocol.....	83
3.6.6	Larval dissection protocol.....	85
3.6.7	Immunostaining protocol for larvae (Fixation, blocking and staining).....	87
	3.6.7(a) Fixation.....	87
	3.6.7(b) Blocking	87
	3.6.7(c) Staining.....	87
3.7	Cell culture	88
3.7.1	Preparation of 1 L M3+BPYE media for DmD8 cells.....	88
3.7.2	DmD8 cells	90
3.7.3	Plasmid transfection.....	90
3.7.4	Immunostaining of DmD8 cells.....	91
3.8	<i>In vitro</i> microtubule co-sedimentation assay	92
3.9	Image acquisition and data analyses	93
3.9.1	Confocal image data acquisition and analysis	93
3.9.2	Dendrite detachment analysis protocol	93
3.10	Protein sequence and multisequence alignment analyses	94
3.11	Graph and statistics	95
	CHAPTER 4 RESULTS	96
4.1	Standardization genetic background of selected <i>Drosophila</i> mutants identified by non-lethal PCR genotyping.....	96
4.2	Role of <i>dystrophin</i> in regulating sensory dendrite morphology.....	113

4.2.1	Heterozygous mutant screen for dendritic morphology changes of C4da neurons	113
4.2.2	Increased dendritic crossings of C4da neurons upon <i>dystrophin</i> RNAi knockdown in epidermal cells.....	119
4.2.3	Dendrite morphology is normal in RNAi knockdown or overexpression of <i>dystrophin</i> in C4da neuron	123
4.2.4	<i>Dystrophin</i> overexpression in epidermal cells aggravates its mutant phenotype	128
4.3	<i>Dystrophin</i> RNAi knockdown in epidermal cells results in ECM detachment of C4da dendrites	132
4.4	Predictive microtubule-binding domain in <i>Drosophila</i> Dystrophin isoforms	138
4.5	Dystrophin overexpression leads to accumulation of inclusion bodies in DmD8 cells and <i>Drosophila</i> larval epidermal cells	140
4.6	<i>Drosophila</i> Dystrophin binds directly to microtubule	150
CHAPTER 5 DISCUSSION		166
5.1	Mutations in <i>Drosophila</i> mutants and genotyping	166
5.2	Uncovering novel epidermal genes related to sensory dendrite morphology	172
5.2.1	Heterozygous mutant screen	172
5.2.2	RNAi knockdown of <i>dystrophin</i> in epidermal cells.....	174
5.2.3	RNAi knockdown or overexpression of <i>dystrophin</i> in C4da neuron.....	175
5.2.4	<i>Dystrophin</i> rescue experiment	176
5.3	Epithelium-ECM interactions in dendrite detachment.....	177
5.4	Dystrophin protein isoform sequence analysis.....	179
5.5	Dystrophin is a microtubule-associated protein	180
5.6	Bacterial produced <i>Drosophila</i> Dystrophin possesses <i>in vitro</i> microtubule-binding activity	182
CHAPTER 6 CONCLUSION, LIMITATIONS OF STUDY AND FUTURE RECOMMENDATIONS		188
6.1	Conclusion.....	188

6.2	Limitations of study	189
6.3	Recommendations for future research.....	190

REFERENCES..... 193

APPENDIX A: PROTEIN CONCENTRATION STANDARD CURVE

APPENDIX B: DP186 CDNA SEQUENCE

APPENDIX C: DP186 PROTEIN ATTRIBUTES AND SEQUENCE

APPENDIX D: EPITHELIAL SPECIFICITY OF *GAL4^{A58}* DRIVER IN LARVAL EPIDERMIS

LIST OF PUBLICATIONS/ PRESENTATIONS

LIST OF TABLES

	Page
Table 2.1	Balancer chromosomes in <i>Drosophila</i> 12
Table 3.1	Media and solutions 45
Table 3.2	Long-term storage of <i>E. coli</i> 45
Table 3.3	Preparation of antibiotics 45
Table 3.4	1% (w/v) agarose gel casting for DNA electrophoresis 45
Table 3.5	DNA gel electrophoresis 45
Table 3.6	<i>E. coli</i> competent cell preparation 45
Table 3.7	Protein expression and purification 46
Table 3.8	Buffer exchange by dialysis 46
Table 3.9	Protein concentration measurement 46
Table 3.10	Sodium Dodecyl Sulphate-Polyacrylamide gel electrophoresis (SDS-PAGE) 46
Table 3.11	Western blot hybridization 47
Table 3.12	Fly husbandry 47
Table 3.13	PCR genotyping protocol 47
Table 3.14	Larval dissection protocol 48
Table 3.15	Immunostaining protocol for larvae 48
Table 3.16	DmD8 cell culture 48
Table 3.17	Immunostaining of DmD8 cells 49
Table 3.18	<i>In vitro</i> microtubule co-sedimentation assay 49
Table 3.19	List of enzymes and antibodies 49
Table 3.20	List of kits 50
Table 3.21	List of consumables 50

Table 3.22	List of general instruments.....	51
Table 3.23	DNAs and plasmids used in this work.....	53
Table 3.24	Genotypes and features of <i>E. coli</i>	58
Table 3.25	Fly stocks	59
Table 3.26	Antibiotics preparation.....	63
Table 3.27	Standard reaction setup for PCR.....	68
Table 3.28	Polymerase Chain Reaction protocol and parameters.....	68
Table 3.29	pCR™ II-Blunt-TOPO Cloning® mixture.....	71
Table 3.30	Ligation mixture for DNA	73
Table 3.31	Stock solution for SDS-PAGE preparation.....	76
Table 3.32	10% acrylamide gel.....	77
Table 3.33	Dilutions of antibodies for Western blotting.....	80
Table 3.34	Lab media for 1 L fly food.....	81
Table 3.35	General reaction mixture for PCR.....	84
Table 3.36	PCR genotyping parameters.....	86
Table 3.37	Big Dye terminator 3.1 reaction mixture for DNA sequencing	86
Table 3.38	Dilutions of antibodies for staining protocol	89
Table 4.1	Designed primers used for mutant genotyping	99
Table 4.2	Designed primers used in construction of truncated <i>Dp186</i> genes..	144
Table 4.3	Designed primers of <i>Dp186</i> used for <i>in vitro</i> experiment.....	153
Table 4.4	The calculated and apparent size of Dp186 truncated proteins expected and migrated on SDS-PAGE	159

LIST OF FIGURES

	Page
Figure 2.1	The life cycle of <i>Drosophila melanogaster</i>7
Figure 2.2	The GAL4-UAS system for directed gene expression in <i>Drosophila melanogaster</i> 10
Figure 2.3	Diagram of neuron 13
Figure 2.4	Microtubule orientations in different neuron types..... 13
Figure 2.5	The four classes (classes I-IV) of <i>Drosophila melanogaster</i> dendritic arborisation neurons..... 15
Figure 2.6	Dendritic morphologies are regulated by intrinsic transcription factors..... 17
Figure 2.7	Positioning of class IV da dendrites and a cross section view of the epidermis20
Figure 2.8	Positioning of class IV da dendrites relative to the ECM.21
Figure 2.9	The Dystrophin-associated protein complex.....23
Figure 2.10	A group of myofibrils connected to the sarcolemma via the costameres.....23
Figure 2.11	The gene structure of human <i>dystrophin</i>24
Figure 2.12	The gene structure of <i>dystrophin</i> in <i>Drosophila</i>26
Figure 2.13	Typical full-length of Dystrophin protein.....28
Figure 2.14	Comparison of Dystrophin and Utrophin.....30
Figure 2.15	Microtubule organization in extensor digitorum longus of 6-month-old mouse.....31
Figure 2.16	Muscle degeneration upon reduction of either all <i>dystrophin</i> isoform or solely the <i>Dp117</i>32
Figure 2.17	Expression of Dp186 in synapse-rich regions of larval neuropiles....34

Figure 2.18	Miniaturized Dystrophin abridged from full-length Dystrophin.	36
Figure 3.1	Experimental design of this study	41
Figure 3.2	Gateway [®] Directional TOPO [®] entry vector used in this study.	54
Figure 3.3	Vector map of pBID-UASC-FG.	55
Figure 3.4	pCR [®] -Blunt II-TOPO [®] vector.	56
Figure 3.5	Bacterial expression vector, pET-47b(+) used protein production in <i>E. coli</i>	57
Figure 4.1	Genetic cross for standardization genetic background of mutants.	98
Figure 4.2	Schematic diagram showing the basic concept of primer designed for deletion mutation mutant and their possible outcomes for different genotypes.	101
Figure 4.3	Primer design of screening for <i>dystrophin</i> mutant files on third chromosome.	101
Figure 4.4	Gel analysis of representative screening for <i>dys</i> ^{Dp186 166.3/+} by PCR genotyping.	102
Figure 4.5	Gel analysis of representative screening for <i>dys</i> ^{E6/+} by PCR genotyping.	104
Figure 4.6	Primer design and experimental workflow for genotyping a single point mutation mutant.	104
Figure 4.7	Representative DNA sequencing results of single point mutation site at <i>Adenomatous polyposis coli</i> gene in <i>APC1</i> ^{Q8/+} heterozygous mutant.	105
Figure 4.8	Representative DNA sequencing results of single point mutation site at <i>Adenomatous polyposis coli</i> gene in <i>APC2</i> ^{g10/+} heterozygous mutant.	105
Figure 4.9	Representative DNA sequencing results of single point mutation site at <i>dystroglycan</i> gene in <i>Dg</i> ^{O43/+} heterozygous mutant.	107
Figure 4.10	Representative DNA sequencing results of single point mutation site at <i>dystroglycan</i> gene in <i>Dg</i> ^{O86/+} heterozygous mutant.	107

Figure 4.11	Representative amplification of genomic DNA fragment containing single point mutation of <i>APCI</i> ^{Q8} by PCR.	108
Figure 4.12	Representative amplification of genomic DNA fragment containing single point mutation of <i>APC2</i> ^{g10} by PCR.	108
Figure 4.13	Amplification of genomic DNA fragment containing single point mutation of <i>Dg</i> ^{O43} by PCR.	109
Figure 4.14	Amplification of genomic DNA fragment containing single point mutation of <i>Dg</i> ^{O86} by PCR.	109
Figure 4.15	Representative DNA sequencing results of screening for <i>APCI</i> ^{Q8/+} flies in backcrossing.	110
Figure 4.16	Representative DNA sequencing results of screening for <i>APC2</i> ^{g10/+} flies in backcrossing.	111
Figure 4.17	DNA sequencing results of screening for <i>Dg</i> ^{O43/+} flies in backcrossing.	112
Figure 4.18	DNA sequencing results of screening for <i>Dg</i> ^{O86/+} flies in backcrossing.	114
Figure 4.19	Genetic cross scheme for generating fly expressing epidermal specific <i>Gal4</i> ^{A58} in background of <i>shotgun-tdTomato</i> and <i>ppk-CD4-GFP</i>	115
Figure 4.20	Live imaging of heterozygous mutant experiment.	116
Figure 4.21	Quantification of heterozygous mutant experiment.	118
Figure 4.22	The location of the deletions in mutants and RNAi knockdown of <i>Drosophila dystrophin</i> gene.	120
Figure 4.23	Live imaging of RNAi knockdown in epidermal cells.	121
Figure 4.24	Quantification of RNAi knockdown in epidermal cells experiments.	122
Figure 4.25	Live imaging of RNAi knockdown and transgenic expression in C4da neuron.	125

Figure 4.26	Quantification of RNAi knockdown and transgenic expression in C4da neuron experiments.....	126
Figure 4.27	Genetic cross scheme for rescue experiment.	129
Figure 4.28	Live imaging of rescue experiments.	130
Figure 4.29	Quantification of rescue experiment.	131
Figure 4.30	Genetic cross for generating fly expressing epidermal specific <i>Gal4^{A58}</i> in background of <i>viking-GFP</i> and <i>ppk-CD4-tdTomato</i>	133
Figure 4.31	Dendrite detachment analysis using <i>viking-GFP</i> and <i>ppk-tdTomato</i> fly line.	134
Figure 4.32	Representative dendrite detachment results in RNAi knockdown...	136
Figure 4.33	Quantitative analysis of dendrite detachment from the ECM in RNAi knockdown.....	137
Figure 4.34	Predictive domain structure of protein isoforms in <i>Drosophila</i>	139
Figure 4.35	Comparison of the amino acid sequences of Dystrophin protein isoforms in <i>Drosophila</i>	141
Figure 4.36	Schematic diagram of the truncated Dp186 domain proteins used in this study.	142
Figure 4.37	Primer design and construction of truncated <i>Dp186</i> domain genes.....	145
Figure 4.38	Expression of truncated Dp186 domain proteins in DmD8 cells probed by immunoblot.	146
Figure 4.39	Immunostaining of Dp186 and microtubules in DmD8 cells.	148
Figure 4.40	Immunostaining epidermis with Dp186 and microtubules in dissected third instar larva.....	149
Figure 4.41	Diagram showing Dp186 domain protein structure designed for microtubule-binding assay.	152
Figure 4.42	1% agarose gel analysis of purified PCR products of <i>Dp186</i>	154
Figure 4.43	Time-course expression of Dp186 domain proteins in <i>E. coli</i> at different temperatures.	156

Figure 4.44	Time-course expression of Dp186 domain proteins in in <i>E. coli</i>	156
Figure 4.45	Optimization expression of C-terminal domain protein of Dp186 at different time points.	157
Figure 4.46	10% SDS-PAGE analysis of the purification of N-terminal domain protein of Dp186 by Ni-NTA system.....	160
Figure 4.47	10% SDS-PAGE analysis of the purification of 4-spectrin repeats domain protein of Dp186 by Ni-NTA system.....	160
Figure 4.48	10% SDS-PAGE analysis of the purification of C-terminal domain protein of Dp186 by Ni-NTA system.....	161
Figure 4.49	10% SDS-PAGE analysis of dialyzed domain proteins of Dp186. .	161
Figure 4.50	10% SDS-PAGE analysis of multi-step gradient dialysis of C-terminal domain protein of Dp186.....	163
Figure 4.51	Experimental controls of microtubule co-sedimentation assay in 10% SDS-PAGE.	164
Figure 4.52	Microtubule co-sedimentation assay of Dp186 domain proteins.....	165
Figure 5.1	The location of the deletion <i>dys^{DLP2 E6}</i> and <i>dys^{Dp186 166.3}</i> on the structure of the <i>Drosophila dystrophin</i> gene of third chromosome.	168
Figure 5.2	Schematic representations of <i>Drosophila</i> APC proteins with the sites of relevant null mutations indicated (APC1 ^{Q8} and APC2 ^{g10}) on third chromosome.....	170
Figure 5.3	Diagram of the same isoform showing the extent of the α and β subunits of the processed proteins, and the positions of the lesions and the change associated with the <i>Dg</i> alleles on second chromosome.....	170
Figure A	Typical protein concentration standard curve using the standard assay protocol with BSA	
Figure D	Epithelial specificity of <i>Gal4^{A58}</i> driver in larval epidermis	

LIST OF SYMBOLS

%	Percentage
°C	Degree Celsius
bp	Base pair
g	Gram
h	Hour
kDa	Kilo Dalton
L	Liter
min	Minute
mg	Milli gram
mL	Milliliter
mM	Milli molar
ng	Nano gram
OD	Optical density
pmol	picomole
psi	Pounds per square inch
T _a	Annealing temperature
T _m	Melting temperature
U	Unit
V	Voltage
w/v	Mass per volume
α	Anti
<i>g</i>	Relative centrifugal force
μL	Micro liter
μg	Micro gram

LIST OF ABBREVIATIONS

APC	Adenomatous Polyposis Coli
APS	Ammonium persulfate
BMD	Becker muscular dystrophy
BSA	Bovine serum albumin
C4da	Class IV dendrite arborization
CO ₂	Carbon dioxide
ddH ₂ O	Double distilled water
Da	Dendrite arborization
DAPC	Dystrophin associated protein complex
DAPI	4',6-diamidino-2-phenylindole
Dg	Dystroglycan
DMD	Duchenne muscular dystrophy
DNA	Deoxyribonucleic acid
dNTP	Deoxyribonucleotide
Dys	Dystrophin
ECM	Extracellular matrix
EDTA	Ethylenediaminetetraacetic acid
EtBr	Ethidium bromide
IPTG	Isopropyl β -D-1-thiogalactopyranoside
LB	Luria Bertani
MAP	Microtubule-associated protein
Ni-NTA	Nickel-nitrilotriacetic acid
PCR	Polymerase Chain Reaction

PHEM	Piperazine-N,N'-bis(2-ethanesulfonic acid) (PIEPS), 4-(2-hydroxyethyl)-1-piperazineethanesulfonic acid (HEPES), ethylene glycol-bis(β -aminoethyl ether)-N,N,N',N'-tetraacetic acid (EGTA), MgSO ₄
RNAi	Ribonucleic acid interference
SDS-PAGE	Sodium dodecyl sulfate - polyacrylamide gel electrophoresis
TAE	Tris-acetate-EDTA
TE	Tris-EDTA
TOR	The target of rapamycin

**PENCIRIAN BOKIMIA DYSTROPHIN TERHADAP DENDRIT
DERIA DAN SEL EPITELIA DALAM *DROSOPHILA MELANOGASTER***

ABSTRAK

Pengelakan/penolakan sendiri antara sentuhan menghadkan dendrit-dendrit saraf deria dalam ruangan 2D. Kecacatan dalam lekatan dendrit-matriks ekstrasel menjejaskan kurungan tersebut dan mengakibatkan silangan sendiri dalam ruangan 3D. Tambahan pula, kompleks-kompleks ini dan kepelbagaian saraf-saraf deria menyulami epidermis dan otot. Walau bagaimanapun, mekanisme yang mengawalatur dendrit-matriks ekstrasel masih kurang difahami. Objektif kajian ini adalah untuk menghurai dan mencirikan gen novel dalam sel epitelia yang mengatur morfologi dendrit saraf-saraf deria dalam larva instar ketiga *Drosophila*. Pertama sekali, latar belakang genetik untuk keturunan mutan yang terpilih: *adenomatous polyposis coli*, *dystroglycan* and *dystrophin* dipiawaikan dengan kacukan balik kepada strain jenis liar dan kemudian dikenalpasti dengan menggunakan kaedah penjenisan gen tindak balas berantai polimerase (PCR) yang tidak maut daripada sayap *Drosophila*. Dalam kajian ini, *dystrophin* dalam sel epitelia ditemui mempelapiki morfologi dendrit saraf-saraf deria dalam larva instar ketiga *Drosophila*. Mutasi atau ketuhan RNAi *dystrophin* dalam sel-sel epidermis menyebabkan peningkatan silangan dendrit saraf-saraf deria. Sebaliknya, fenotip morfologi dendrit normal dipamerkan apabila ketuhan RNAi atau *dystrophin* pengekspresan transgen dalam saraf. Adalah mengejutkan bahawa pengekspresan transgenik *Dp186 dystrophin* dalam sel-sel epidermis bertambah buruk terhadap fenotip mutannya, bukan menyelamatkannya. Analisis lekatan dendrit-matriks ekstrasel dengan mikroskopi sefokus leraian tinggi dan penanda label berpendarfluor

dalam larva instar ketiga *Drosophila* menyokong bahawa pengurangan *dystrophin* dalam sel epidermis menggalakkan dendrit terpisah daripada ECM. Analisis komputasional meramalkan majoriti isoform Dystrophin mengadungi domain pengikatan mikrotubul, yang bertanggungjawab untuk pengikatan mikrotubul secara langsung. Analisis imunopendarfluor sel DmD8 dan sel epidermis larva memerhatikan penempatan mikrotubul-mikrotubul dengan Dp186 Dystrophin, namun Dp186 Dystrophin yang tanpa domain pengikatan mikrotubul tidak bersekutu dengan mikrotubul. Di sini, keputusan *in vivo* adalah tidak muktamad yang disebabkan oleh masalah teknikal: pembentukan jasad rangkuman oleh pengekspresan Dp186 Dystrophin yang terlebih dan kuasa mikroskopi sefokus yang terhad. Walau bagaimana pun, asai *in vitro* mengesahkan bahawa Dp186 Dystrophin hasilan bakteria mengikat mikrotubul secara langsung melalui domain pengikatan mikrotubul. Pada masa depan, kajian yang lebih mendalam diperlukan untuk menjelaskan peranan Dystrophin dalam penyelarasan pembentukan ranting dendrit deria.

**BIOCHEMICAL CHARACTERISATION OF DYSTROPHIN IN
SENSORY DENDRITE AND EPITHELIAL CELLS OF *DROSOPHILA
MELANOGASTER***

ABSTRACT

Contact-mediated self-avoidance/repulsion restricts dendrites of sensory neuron in a 2D space. Defect in dendrite-extracellular matrix (ECM) adhesion disrupts the confinement and results in self-crossing of dendrites in a 3D space. In addition, these complex and diverse patterns of sensory neurons innervate the epidermis and muscle. However, the mechanisms governing dendrite patterning are still poorly understood. The objectives of this study are to uncover and characterise a novel gene in epithelial cells regulating dendritic morphology of sensory neurons in *Drosophila* third instar larvae. First of all, the genetic background of selected *Drosophila* mutant lines: *adenomatous polyposis coli*, *dystroglycan* and *dystrophin* was standardized by backcrossing to the wild type strain and then identified by using non-lethal PCR genotyping method from *Drosophila* wings. In this study, *dystrophin* in epithelial cells was found underlying the dendritic morphology of sensory neurons in *Drosophila* third instar larvae. Mutations or RNAi knockdown of *dystrophin* in epidermal cells were led to an increase in dendritic self-crossing of sensory neurons. In contrast, normal phenotype of dendrite morphology was exhibited upon RNAi knockdown or transgenic expression of *dystrophin* in neurons. Surprisingly, transgenic expression of *dystrophin Dp186* in epidermal cells exacerbated its mutant phenotype, instead of rescuing it. Analysis of dendrite-ECM adhesion with high-resolution confocal microscopy and fluorescent-labelled markers in third instar larva corroborated that the reduction of *dystrophin* in epidermal cells promoted dendrites

to be detached from the ECM. Computational analysis predicted the majority of Dystrophin isoforms contained microtubule-binding domain, which was responsible for direct binding of microtubules. Immunofluorescence of DmD8 cells and larval epidermal cells of *Drosophila* observed a colocalization of Dystrophin Dp186 and microtubules, but devoid of microtubule-binding domain of Dystrophin Dp186 did not associate with microtubules. Here, *in vivo* results were inconclusive due to technical problems: inclusion body formation by overexpression of Dystrophin Dp186 and the limited resolution power of confocal microscopy on microtubules. However, *in vitro* assay confirmed that bacterial produced Dystrophin Dp186 binds microtubules directly through its microtubule-binding domain. In future, further in-depth study is required to elucidate the role of Dystrophin in coordinating sensory dendrite arborization.

CHAPTER 1

INTRODUCTION

1.1 Background of study

Neurons are the basic units of the nervous system and responsible to transmit information received from dendrites and then relayed electrical signals to others through axons. Dendrites of neurons possess distinct morphologies to receive input of sensory cues (Corty *et al.*, 2009; Arikath, 2012). In this context, the highly stereotyped organization of the dendritic arborisation (da) neurons in *Drosophila* peripheral nervous system (PNS) are useful to study the dendritic morphology and the underlying mechanism shaping the dendrites.

Patterning of da sensory neurons in the *Drosophila* peripheral nervous system (PNS) requires contact-mediated self-avoidance and tiling of dendrites. Self-avoidance between dendrites is mediated by cell-surface receptor Dscam, a vast variety number of transmembrane immunoglobulin (Ig) proteins generated by alternative splicing (Matthews *et al.*, 2007). Dendritic tiling, controlled by several genes, establishes a non-overlapping coverage of dendritic receptive fields (Emoto *et al.*, 2004; Emoto *et al.*, 2006; Koike-Kumagai *et al.*, 2009). The classification of da sensory neuron is based on complexity of dendritic morphology and regulated by combinatorial intrinsic transcription factors (Parrish *et al.*, 2007; Jan and Jan, 2010). However, orchestration of dendritic patterning requires a flat 2D environment provisioned by dendrite-ECM adhesion.

Latest studies have begun to reveal that the dendrite-ECM adhesion is regulated by underlying epidermal cells, via secretion of substances into ECM. Epidermis-derived heparan sulphate proteoglycans in ECM was shown to act as a

local permissive signal for the growing of space-filling nociceptive C4da neurons (Poe *et al.*, 2017). Neuronal integrins interact with epidermis-derived laminins in the ECM to adhere dendrite on the basal surface of epidermal cells (Kim *et al.*, 2012) in contact with the ECM. The dendrite adhesion is also mediated by interacting of dendritic Ret receptors with integrins (Soba *et al.*, 2015). However, loss of semaphorin ligand from epidermis leads to a defect in the adhesion (Meltzer *et al.*, 2016). The defect of dendrite-ECM adhesion causes dendrites to be detached from the ECM and enclosed by underlying epidermal cells, resulting in excessive non-contacting self-crossings between dendrites. Under normal circumstance, the dendrite enclosure by septate junction protein, coracle, was shown to restrict branching and permit coordinated development of spatially overlapping sensory (Tenenbaum *et al.*, 2017).

Besides, sensory neurons have recently been found to be defined by the interplay between epidermal cells and muscles, where positional cues are relayed to hypodermal cells to guide sensory dendrite outgrowth in *C. elegans* (Liang *et al.*, 2015). SAX-7 stripes, sarcomere-like pattern stripes on the hypodermal cell surface constituted of a tripartite complex: SAX-7, a hypodermal trans-membrane adhesion molecule, DMA-1 (trans-membrane LRR neuronal protein receptor in multidendritic PVD neuron) and MNR-1 (a novel membrane protein), spatially instruct dendrite outgrowth of *C. elegans* PVD 4°C neuron growing between the muscle and hypodermis. PVD 4°C neuron functions as a body mechanosensory neurons responding to harsh mechanical stimuli and cold temperature (Way and Chalfie, 1989; Chatzigeorgiou *et al.*, 2010). In pre-patterning these dense parallel stripes, the tripartite complex is distributed in mutually exclusive fashion with longitudinally aligned UNC-52/Perlecan, a heparin sulphate proteoglycan at the basement

membrane tethered to muscle by integrin complexes, thereby SAX-7 stripes are intercalated between UNC-52 motifs (Liang *et al.*, 2015).

Interestingly, epidermal epithelial cells, rather than hemocytes, also function to clear the degenerating dendrites via Draper-mediate recognition (Han *et al.*, 2014). In addition, dendrite regeneration of adult *Drosophila* sensory neurons after injury is facilitated by surrounding extracellular matrix, but it is inhibited by epidermal-derived matrix metalloproteinase 2 (MMP2) (DeVault *et al.*, 2018).

1.2 Statement of problem

The complex and diverse patterns of somatosensory neurons innervate the epidermis and muscle, but the extrinsic cues relayed from environment governing dendrite outgrowth and patterning of sensory neuron still remain unknown. More important, the complex relationship between dendrites, the extracellular matrix (ECM) and epidermal cells remains an interesting question to be answer. In addition, the signalling cascade initiated by environmental cues in regulating the growth of dendrites has not been defined (Jiang and Parrish, 2015).

1.3 Hypothesis

Dystrophin in epithelial cells is predicted underlying the dendritic morphology of sensory neurons in *Drosophila* third instar larvae.

1.4 Rationale of study

Dendrite positioning and patterning of sensory neurons require the complex interaction between dendrite and epidermal cells. Several important cues in epidermal cells have recently been found underlying dendrite morphology in

Drosophila (Han *et al.*, 2012; Kim *et al.*, 2012; Jiang *et al.*, 2014; Meltzer *et al.*, 2016). The rationales of this study are to identify and characterise a new gene in epithelial cells regulating dendrite positioning and patterning using genetic screen, computational analysis and biochemical analysis in *Drosophila*. The significance of the study will provide a new insight and understanding into the complex interaction between dendrite, ECM and epidermis in *Drosophila*.

First of all, the genetic background of *Drosophila* mutants for selected candidate genes was standardized to wild type control strain by backcrossing and then identified by non-lethal PCR genotyping. This method in principle is to minimize and dampen the confounding effects of genetic background variability (Linford *et al.*, 2013). Then, rapid heterozygous mutant screen and RNAi knockdown assay were performed on the standardized *Drosophila* mutants in order to identify candidate genes affecting dendrite morphology of sensory neurons in *Drosophila* larvae. The exhibited dendritic phenotype of sensory neurons was further analysed by dendrite detachment analysis in order to investigate the spatial distribution of dendrites in relation to the ECM. Here, the interested candidate gene was analysed by *in silico* multiple sequence alignment analysis to study the closely related gene isoforms produced in *Drosophila*.

Finally, the candidate gene was characterized by *in vitro* microtubule-binding assay and *in vivo* assay by expressing in DmD8 cells and epidermal cells of *Drosophila* larval epidermal cells in order to study its potential intrinsic property and spatial distribution in cells, respectively.

1.5 General and specific objectives

1.5.1 General objectives

The general objectives of this study are to uncover and characterise a new gene in epithelial cells regulating dendritic morphology of sensory neurons in *Drosophila* larvae.

1.5.2 Specific objectives

1. To standardize the genetic background of candidate *Drosophila* mutants identified by non-lethal PCR genotyping
2. To screen and identify candidate genes affecting dendritic morphology of sensory neurons in *Drosophila* larvae through heterozygous mutant screen and RNAi knockdown assay
3. To examine dendritic crossing phenotype of sensory neurons upon *dystrophin* RNAi knockdown in epidermal cells by dendrite detachment analysis
4. To analyse dystrophin protein *in silico* by multiple sequence alignment analysis, and characterize *itin vitro* by microtubule binding assay and *in vivo* by expressing in DmD8 cells and *Drosophila* larval epidermal cells.

CHAPTER 2

LITERATURE REVIEW

2.1 *Drosophila melanogaster*

2.1.1 Introduction

Fruit flies are small, short life-span, inexpensive and relatively easy to be reared on simple food comprised of sucrose, yeast and a weak organic acid as preservative in the laboratory (Roote and Prokop, 2013; Piper *et al.*, 2014). Because of these features, Thomas Hunt Morgan use fruit flies to investigate the chromosomal theory of inheritance. More important, it has only four pairs of chromosomes and no meiotic recombination in males. However, it has to be continuously maintained in the laboratory because it is impossible to be stored at cold temperature (St Johnston, 2002; Roote and Prokop, 2013).

2.1.2 *Drosophila* life cycles

At 25°C, *Drosophila melanogaster* takes about ten days to complete its life cycle (Figure 2.1). Freshly laid fertilized egg takes about 21 hour for embryonic development and then hatches into first instar larvae. Transition from first instar into second and third instar larva takes two days. The third instar larvae spends another two days for feeding before wandering away from food to form pupae. During the pupal stage, all organs undergo histolysis and restructure into adult shapes. After about four to five days, adult fly emerges from the pupal case and stay as a virgin for up to eight hours. *Drosophila* life cycle is sensitive to husbandry temperature. It can

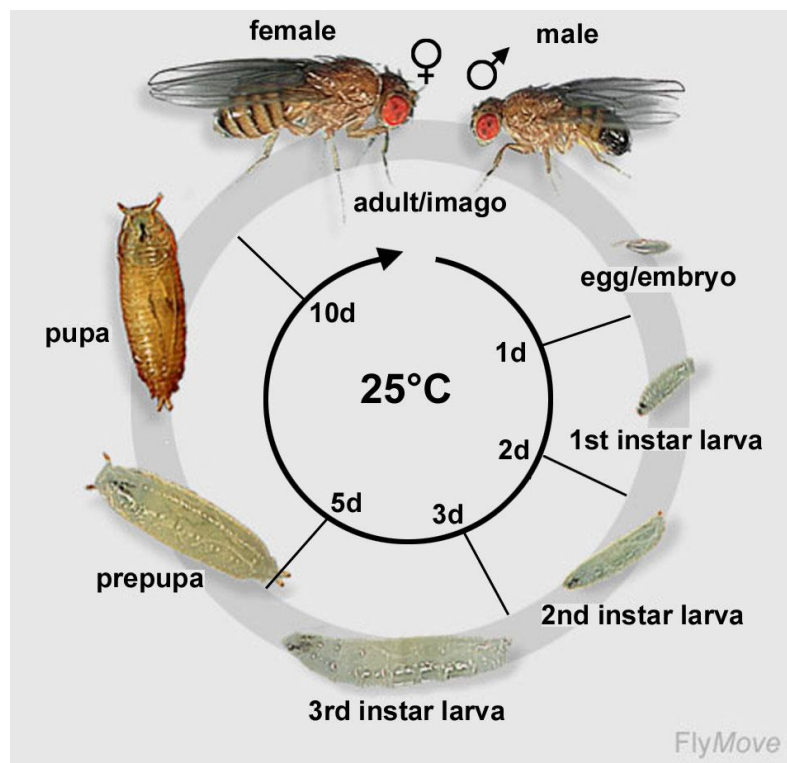


Figure 2.1 The life cycle of *Drosophila melanogaster* (Adapted from Roote and Prokop, 2013)

grow faster minimal for seven days at 29°C or slower maximal for 19 days at 18°C (Roote and Prokop, 2013).

2.1.3 GAL4-UAS system in *Drosophila*

The GAL4-UAS system is one of the powerful tool or popularly to be known as fly geneticist's Swiss army knife for targeted gene expression in *Drosophila* (Brand and Perrimon, 1993). Targeted gene expression in a temporal and spatial manners is one of the most powerful tools to characterize gene function in *Drosophila* (Duffy, 2002) as compared to other two methods: heat shocking method using heat shock promoter and driving expression using endogenous tissue-specific promoters (Brand and Perrimon, 1993). Although heat shocking method allows heat inducible expression, but its ubiquitous and basal expressions can induce phenocopies. Endogenous tissue-specific promoters are indeed very useful to restrict gene expression to a defined subset of cells, however, their selections are limited to characterized promoters and toxicity of target gene product (Brand and Perrimon, 1993).

Initially, Brand and Perrimon (1993) created this system to direct targeted expression on development of *Drosophila* based on the non-toxic effect of the expression of GAL4 in *Drosophila*. GAL4 encodes 881 amino acids of protein, which is identified in the yeast *Saccharomyces cerevisiae* as a regulator of galactose-induced genes. It regulates the transcription of *GAL1* and *GAL10* genes by directly binding to four related 17 bp sites located between these loci or known as *Upstream Activating Sequence (UAS)* element (Duffy, 2002). Capability of GAL4 acting as a

transcription regulator is not only limited to *Drosophila*, but it also performs a similar function in wide variety of other systems as well (Duffy, 2002).

In *Drosophila*, this binary expression system is segregated into two parental parts: enhancer-trap GAL4 driver line and UAS (Upstream Activation Sequence) responder line (Figure 2.2). The yeast transcriptional activator GAL4 is expressed under the control of hijacked nearby genomic enhancers. Binding of GAL4 to UAS element of P-element integration based vector (pUAST) in progeny allows the expression of responder gene from *heat shock protein 70* (*hsp 70*) basal promoter and the SV40 small t intron, and transcription required polyadenylation signal (Duffy, 2002). Temperature dependence of GAL4 activity adds to this flexibility feature by simply altering the rearing temperature to tune the expression levels of responder of gene. The minimal activity of GAL4 is present at 16°C, whereas higher temperature at 29°C offers a balance of maximal GAL4 activity and minimal effect on fertility and viability (Duffy, 2002). This powerful system can express desired gene in tissue or cell specific method (St Johnston, 2002). In *Drosophila* cell culture, cotransfection of UAS responder constitutive drivers, such as Act5-GAL4, allow continual transcription of responder gene. In contrast, inducible responder expression can be achieved with a copper inducible GAL4 under the control of the metallothionein promoter (Duffy, 2002).

2.1.4 Balancer chromosomes

Balancer chromosomes are important genetic tools to maintain deleterious mutations of fly stock and very useful for genetic mating scheme. Balancer chromosomes have three essential features: recessive deleterious mutations,

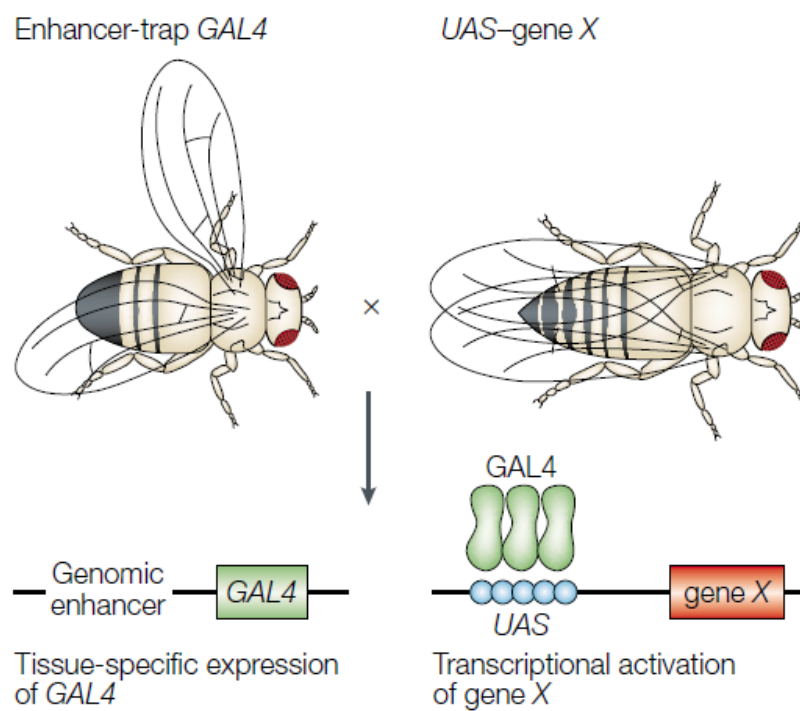


Figure 2.2 The GAL4-UAS system for directed gene expression in *Drosophila melanogaster* (Adapted from St Johnston, 2002)

inversion breakpoints and the presence of genetic marker. Recessive deleterious mutations ensure only heterozygous progeny survive. Inversion breakpoints suppress recombination between sister chromosomes. The presence of genetic marker allows easy recognition the presence of balancer chromosomes (Roote and Prokop, 2013). The example of balancer chromosomes is shown in Table 2.1.

2.2 Neurons and dendrites

Neurons are the fundamental units of the nervous system and the longest cells in body as long as a meter. Most neurons are postmitotic cells and have a limited capability to repair after injury (Martini, 2004). A typical neuron is a highly polarized cell that consists of large cell body (soma) with nucleus, dendrites and an axon (Figure 2.3). Neuron transmits information receiving from dendrites to other cells through its axon in an electrical impulse form (Martini, 2004).

Dendrites are distinguished from axons anatomically and functionally. Structurally, dendrites have tapering processes, whereas axons tend to be very long and slender and are known as nerve fibers (Jan and Jan, 2010). Contrary to axon, dendrites have a small membranous protrusion (dendritic spine), which function to receive input from other cells (Jan and Jan, 2010). In term of the cellular apparatus, Golgi outposts exist primarily in dendrites, not in axon (Horton and Ehlers, 2003). In addition, microtubules in vertebrate and invertebrate dendrites have mixed orientation and are considered a signature of dendrite, whereas microtubules in axon have uniform orientation with their plus ends distal to the cell body (Figure 2.4) (Stone *et al.*, 2008; Rolls and Jegla, 2015). These different cytoskeletal arrangements are related to the cargo transport along axon and dendrites (Jan and Jan, 2010).

Table 2.1 Balancer chromosomes in *Drosophila* (Roote and Prokop, 2013)

Balancer chromosome	Characteristics
<i>FM7a</i> (First multiply-inverted 7a)	X chromosome typical markers: <i>y</i> , <i>wa</i> , <i>sn</i> , <i>Bl</i>
<i>FM7c</i> (First multiply-marked 7c)	X chromosome typical markers: <i>y</i> , <i>sc</i> , <i>w</i> , <i>oc</i> , <i>ptg</i> , <i>Bl</i>
<i>CyO</i> (Curly derivative of Oster)	2 nd chromosome typical markers: <i>Cy</i> (Curly), <i>dp</i> (dumpy; bumpy notum), <i>pr</i> (purple; eye colour), <i>cn2</i> (cinnabar; eye colour)
<i>SM6a</i> (Second multiply-inverted 6a)	2 nd chromosome typical markers: <i>al</i> , <i>Cy</i> , <i>dp</i> , <i>cn</i> , <i>sp</i>
<i>TM3</i> (Third multiply-inverted 3)	3 rd chromosome typical markers: <i>Sb</i> , <i>Ubxbx-34e</i> , (bithorax; larger halteres) <i>e</i> , <i>Ser</i>
<i>TM6B</i> (Third multiply-inverted 6B)	3 rd chromosome frequent markers: <i>AntpHu</i> , <i>e</i> , <i>Tb</i> (Tubby; physically shortened 3 rd instar larvae and pupae)

Note that the fourth chromosome does not require balancers since it does not display recombination.

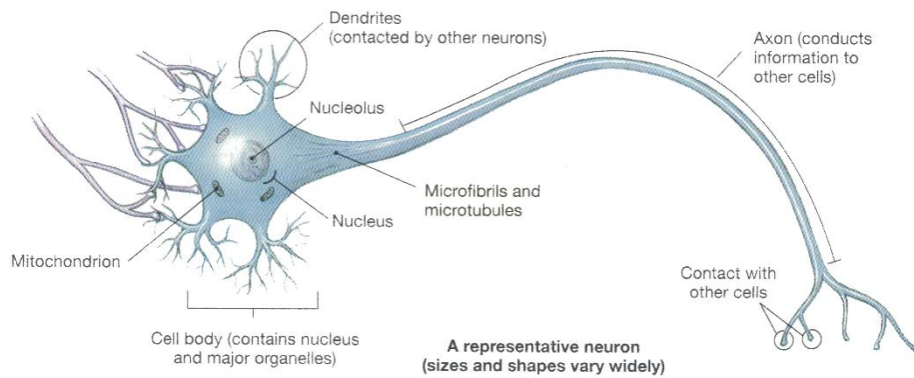


Figure 2.3 Diagram of neuron (Adapted from Martini, 2004)

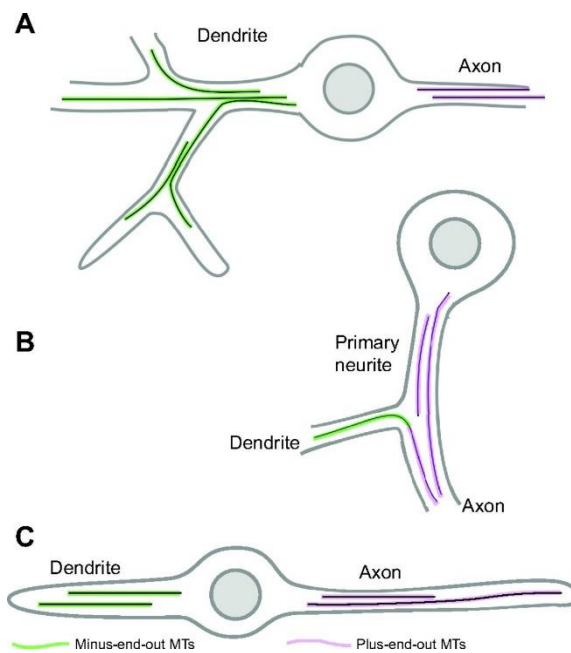


Figure 2.4 Microtubule orientations in different neuron types. (A) *Drosophila* sensory neuron, (B) *Drosophila* motor neurons and interneurons, and (C) *Caenorhabditis elegans* motor neurons. MT, microtubule (Adapted from Rolls and Jegla, 2015).

2.3 *Drosophila* dendrites

The dendritic arborisation (da) sensory neurons of the *Drosophila* larval peripheral nervous system (PNS) are powerful genetic model system to study the molecular mechanisms underlying dendrite-ECM adhesion. *Drosophila melanogaster* features with several attractive attributes: the availability of powerful genetic tools in fruit fly, dendrites of da neurons extending mainly in a 2D plane beneath optically translucent larval cuticle and the stereotypical morphology of distinct classes of da neurons for morphometric analysis (Karim and Moore, 2011).

The larval PNS is comprised of a well-defined array of sensory neurons occupying in each hemisegment (Figure 2.5). Some PNS neurons have single dendrite like external sensory neurons and chordotonal neurons, and some have more extensively branched arbors like the multidendritic neurons (Corty *et al.*, 2009). There are four main da neuron classes (classes I-IV) of *Drosophila* sensory neurons based on dendritic morphologies and central projections as shown in Figure 2.5 and 2.6 (Grueber *et al.*, 2002; Grueber *et al.*, 2007). Classes I-IV are described in order of increasing arbor complexity (Grueber *et al.*, 2002).

Class I neurons, containing vpda, ddaD and ddaE, innervates the larval dorsal region and a restricted ventral region of each hemisegment. Class I neurons are characterized with few side branches and have the least complex dendritic branching (Grueber *et al.*, 2002). Class II neurons, including vda, vdaC, IdaA and ddaB, innervate most of the ventral region of each hemisegment and parts of the lateral and dorsal body wall. Class II neurons feature with long and winding and about symmetrically bifurcating dendrites (Grueber *et al.*, 2002). Class III neurons, comprising of vdaD, v'pda, IdaB, ddaA and ddaF, which occupy about 70% of each abdominal hemisegment territories by long primary and secondary branches of

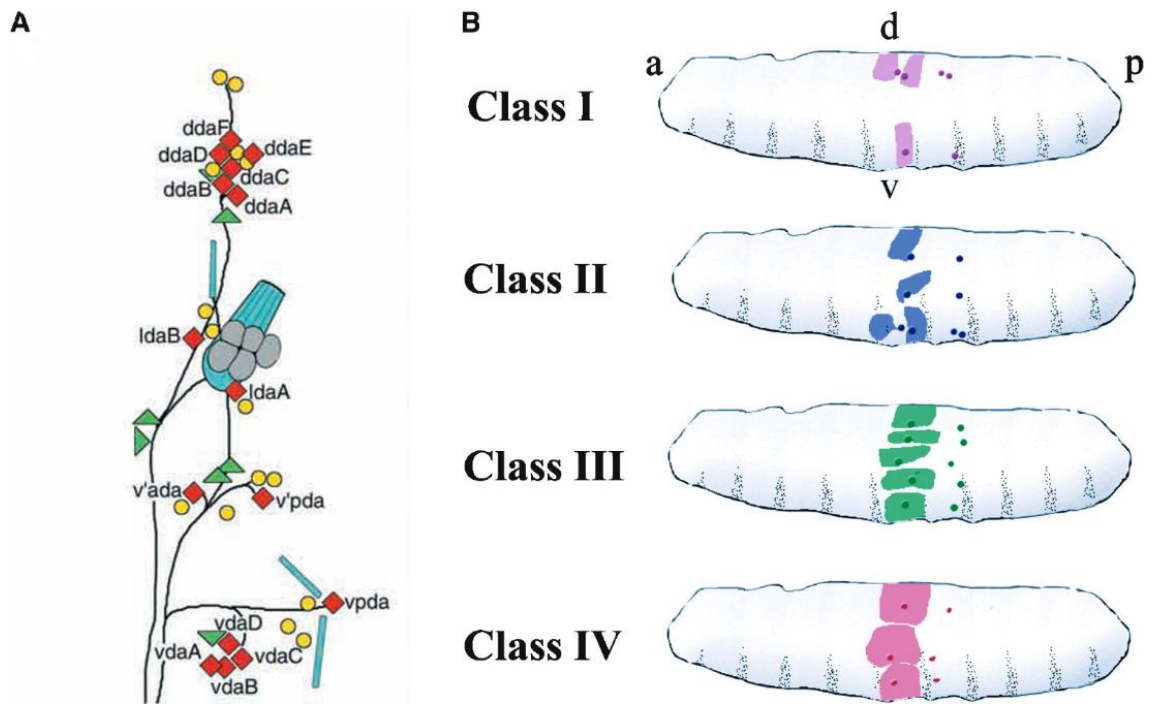


Figure 2.5 The four classes (classes I-IV) of *Drosophila melanogaster* dendritic arborisation neurons. (A) A single abdominal hemisegment, in which the same classes of da neurons are shaded with the same color. da neurons, red diamonds; external sensory neurons, yellow circles; other multidendritic neurons, green triangles; chordotonal organs, blue rectangles. The lateral oenocytes are displayed as gray ovals. The names for the dorsal cluster neurons are designated on the basis of their typical ventral to dorsal cell body position (Adapted from Grueber et al., 2002). (B) The territories (dendritic fields) occupied by different da neuron classes in an abdominal hemisegment. Only two segments are depicted here. a, anterior; p, posterior; v, ventral; d, dorsal (Adapted from Grueber et al., 2003a).

dendrites that are identical to class II dendrites. However, class III dendrites possess dendritic spikes along their length and more complex dendritic branching than class II (Grueber *et al.*, 2002). Class IV neurons, including vdaB, v'ada and ddaC, achieve almost 100% segmental coverage of larval body wall with arbors and are the most complex dendrites. Class III and class IV da neurons display tiling phenomenon, which relies on intrinsic self-avoidance mechanism, to cover larval body walls completely and non-overlappingly (Grueber *et al.*, 2002).

In the functional sensory system, class I neurons act as proprioceptors, sensing muscle contractions, and provide feedback to the CNS signal to coordinate larval locomotion (Hughes and Thomas, 2007). Class II and class III neurons are gentle touch sensors of *Drosophila* larvae and sufficiently to elicit behavior touch responses (Tsubouchi *et al.*, 2012). Multimodal class IV neurons function as nociceptive neurons, detecting noxious heat and noxious heat and noxious mechanical stimuli (Hwang *et al.*, 2007; Xiang *et al.*, 2010). Recently, class IV neurons are discovered to become more complex and hyperarborized when larvae is fed on a protein-deprived food, thereby class IV neurons are hypothesized being able to sense protein-deficient stress (Watanabe *et al.*, 2017).

2.4 Transcriptional control of dendritic morphology

Dendritic arborization (da) neuron classes are regulated by a defined combination of transcription factors as shown in Figure 2.6. EBF transcription factor Knot (also known as Collier) is absolutely expressed in class IV only (Jinushi-Nakao *et al.*, 2007). However, Cut homeodomain protein expression level is widely ranged from nil to high in da neurons: nil in class I, weak in class II, high in class III and intermediate in class IV (Grueber *et al.*, 2003a).

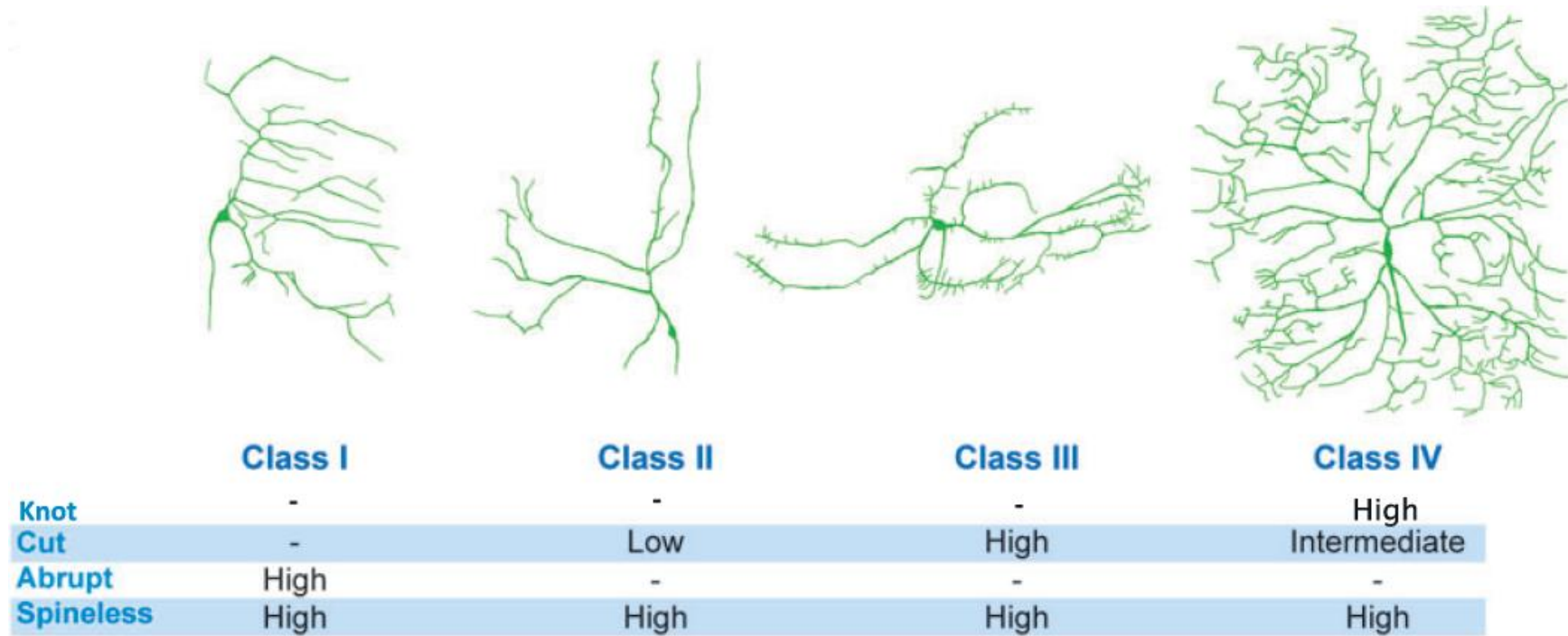


Figure 2.6 Dendritic morphologies are regulated by intrinsic transcription factors. Dendritic morphologies are regulated by intrinsic transcription factors. Stereotyped dendritic morphology of class I, II, III and IV da sensory neurons in the *Drosophila* PNS are correlated with the relative expression levels of the transcription factors Knot, Cut, Abrupt and Spineless in these neurons (Adapted from Parrish et al., 2007; Corty et al., 2009).

Functionally, Knot represses the Cut-induced formation of actin-rich dendritic protrusions (e.g. dendritic spikes in class III neurons) and promotes arbor outgrowth by inducing expression of the microtubule-severing protein Spastin, which promotes dendritic branching by providing short microtubules for invasion at putative branch-points (Jinushi-Nakao *et al.*, 2007; Moore, 2008).

The expression of BTB-Zinc finger protein, Abrupt suppresses branch formation through Centrosomin, which organizes dendritic microtubule nucleation to Golgi outposts in order to repress anterograde microtubule polymerization in termini (Sugimura *et al.*, 2004; Li *et al.*, 2004; Yalgin *et al.*, 2015). Therefore, Abrupt is only expressed in class I neurons, which demonstrate a simple dendritic abors (Parrish *et al.*, 2007). Contrast to Abrupt, the bHLH-PAS protein Spineless is highly expressed in all four classes of da neurons and is essential for the diversification of their dendrite morphology (Kim *et al.*, 2006; Jan and Jan, 2010). Together, these transcription factors finely delineate final morphology of distinct classes of neurons.

2.5 The larval body wall

In *Drosophila*, the outer layer of larval body wall is constituted of a monolayer of terminally differentiated epidermal cells. Its function is equivalent to vertebrate keratinocytes: the first layer of protection barrier against the external insidious environment. In addition, *Drosophila* larval epidermis can secrete a cuticle that functionally equivalent to the stratum corneum of the vertebrate skin (Burra *et al.*, 2013). The tough and waterproof layer is important for maintaining the structural integrity of the larval body. Basal lamina separates epidermal cells from the underlying hemolymph of the larval open circulatory system (Burra *et al.*, 2013).

In *Drosophila*, each abdominal hemisegment of the larva is entirely covered by three class IV da neurons: the dorsal ddaC, the ventro-lateral v'da and the ventral vdaB (Figure 2.7 A) (Han *et al.*, 2012). *Drosophila* class IV dendritic arborisation (da) neurons extend their dendrites between the basal surface of epidermal cells and the extracellular matrix (ECM) (Figure 2.7 B) secreted by the epidermis to tile the larval body wall (Han *et al.*, 2012; Kim *et al.*, 2012). ECM is comprised of many families of molecules including proteoglycans, glycosaminoglycans, collagens and non-collagenous glycoproteins. These glycosylated proteins render the structure and anchorage for cells, outline tissue borders, modulate the extracellular signals and mediate intercellular communication (Reichardt and Prokop, 2011). Transmembrane receptors of ECM, comprising of integrins, syndecans and the Dystrophin-associated glycoprotein complex, are major determinants of cellular structure and intercellular signalling processes (Bokel and Brown, 2002; Hacker *et al.*, 2005; Waite *et al.*, 2009; Broadie *et al.*, 2011).

Transmission Electron Microscopy (TEM) analysis by Han *et al.* (2012) study as shown in Figure 2.8 A of dendrite-epidermal interface revealed that most of dendrites are located beneath the basal surface of epidermal cells and anchored to a scaffolding structures, extracellular matrix (ECM). However, enclosed dendrites are detached from ECM and completely covered by the epidermal cell membrane inside the epidermal cells (Figure 2.8 B), indicating that dendrites can also grow by burrowing into epidermal cells. These enclosed dendrites may appear to cross other branches attached to the ECM in XY-plane (Figure 2.8 C), but in fact the overlapping dendrites are located at different depths of Z-axis and are not in direct contact with each other (Figure 2.8 D). On a 3D sheet of ECM, most class IV da dendrites are anchored to the ECM, except the enclosed dendrites (Figure 2.8 E).

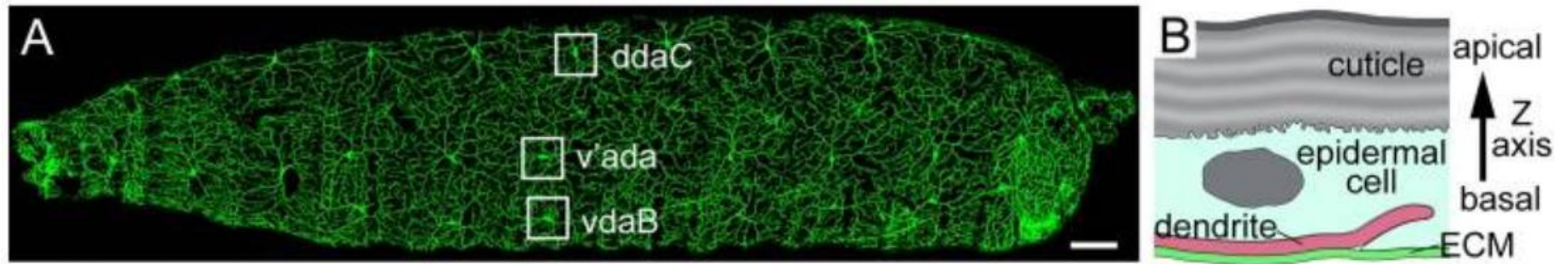


Figure 2.7 Positioning of class IV da dendrites and a cross section view of the epidermis. (A) Class IV da neurons completely and non-redundantly cover the entire body wall with dendritic arbors in a second instar larvae. Scale bar, 10 μ M. (B) Dendrites of class IV are confined between epidermal cell and ECM. The tip of the terminal dendrite is illustrated to extend into the epidermal cell (Adapted from Han et al., 2012).

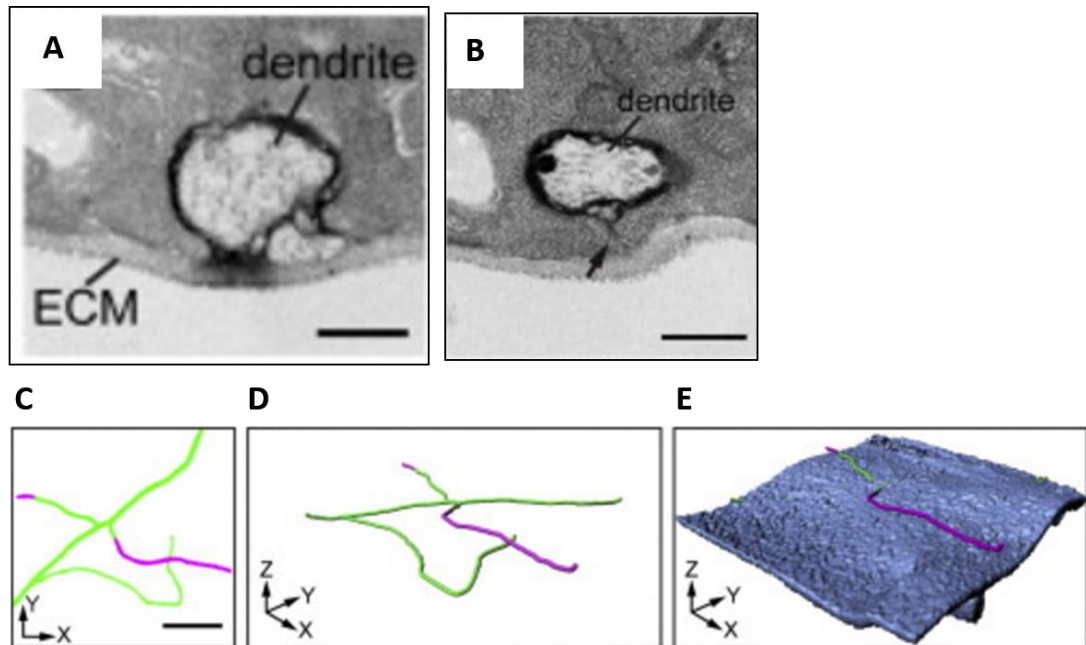


Figure 2.8 Positioning of class IV da dendrites relative to the ECM. TEM images show dendrite are attached to the ECM (A) and enclosed in the epidermal cell layer (B) in cross sections of the larval body wall. The arrow in (B) points to the channel formed by the basal cell membrane of the epidermal cell. Indirect contact of two crossing dendrites in a 2D view (C) and 3D renderings (D and E). The dendrites attached the EMC are in green and the enclosed dendrites are in magenta. The surface rendering of the ECM is in blue. Scale bars, 500 nm (Adapted from Han et al., 2012).

2.6 Dystrophin: An important component of cell membrane

Dystrophin is a rod shaped peripheral membrane protein that functions as a structural link to connect the intracellular cytoskeleton to the extracellular matrix. It is one of the core components of *dystrophin*-associated protein complex (DAPC), including dystroglycans, sarcoglycan complex, α -dystrobrevins, syntrophins, nNOS, and laminin 2 as shown in Figure 2.9. In muscle, DAPC acts as a costamere (Figure 2.10) to stabilize the sarcolemma during the muscle activity and transmitting force generated from muscle sarcomeres to the extracellular matrix. Dystrophin-specific polyclonal antibodies reveal human Dystrophin has 400 kDa molecular weight and occupies merely 0.002% of total striated muscle protein (Hoffman *et al.*, 1987). In addition, DAPC is involved in cell signalling via its interactions with nNOS (Ehmsen *et al.*, 2002).

2.7 Transcription of *dystrophin* gene in human

Dystrophin gene is the longest human gene with 2.5 Mbp of DNA on the locus p21 of X chromosome and comprises of ~1% of its chromosome DNA (Kenrick *et al.*, 1987; Koenig *et al.*, 1987) as shown in Figure 2.11. This large gene comprising of 79 exons and spanning multiple large introns takes 16 hours to be transcribed (Tennyson *et al.*, 1995). Several different isoforms of *dystrophin* are identified and their presence are attributed to the tissue-specific promoters and the alternative splicing events (Feener *et al.*, 1989; Bies *et al.*, 1992; Surono *et al.*, 1997). Principally, transcription of human *dystrophin* gene isoforms (Figure 2.11) is independently regulated by three separate promoters: the brain (B), muscle (M) and Purkinje (P).

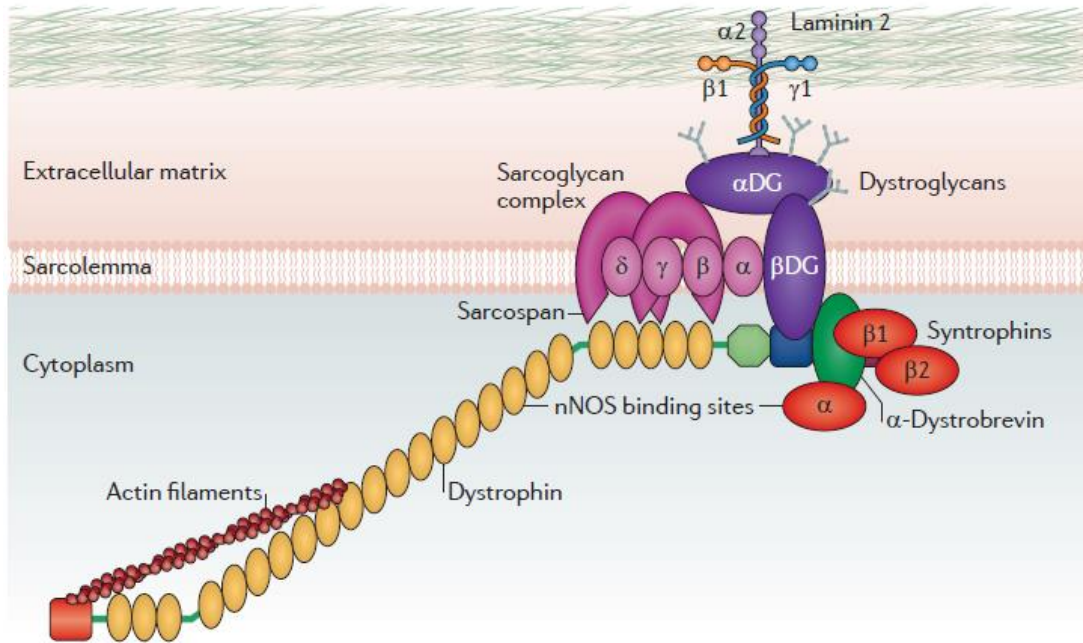


Figure 2.9 The Dystrophin-associated protein complex. Dystrophin links the internal cytoskeleton to the extracellular marix. nNOs, neuronal nitric oxide; α DG, α -dystroglycan; β DG, β -dystroglycan (Adapted from Fairclough et al., 2013).

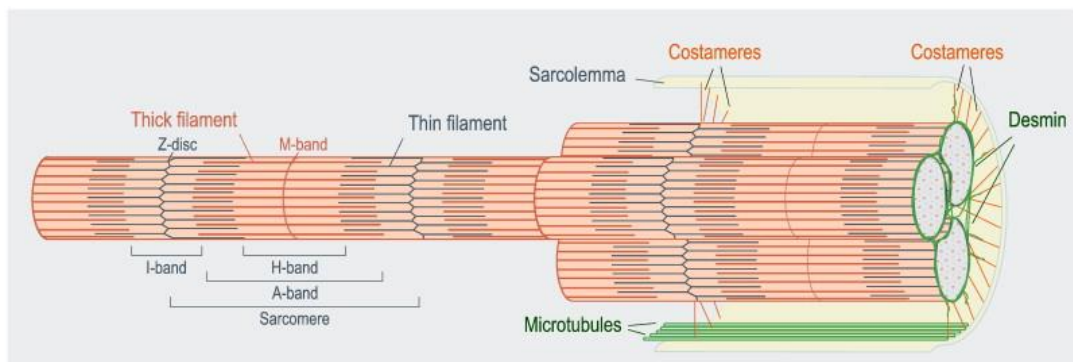


Figure 2.10 A group of myofibrils connected to the sarcolemma via the costameres. Sarcomere is the basic unit of striated muscle tissue, which is located between the borders of Z-dics (Sequeira et al., 2014).

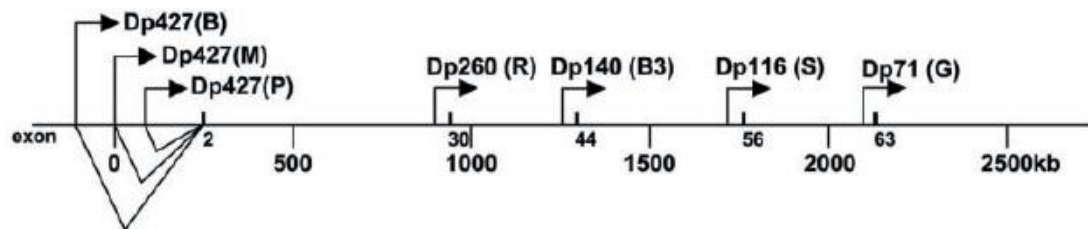


Figure 2.11 The gene structure of human *dystrophin*. The gene size is 2.5 Mb and encodes for 7 different protein isoforms that are driven by their own promoters (arrow) in tissue-specific manners. Three different long isoforms of Dp427 are expressed in brain, muscle and cerebellar Purkinje cells. The other short isoforms are derived from internal promoters. R, retina; B, brain; S, Schwann cells; G, ubiquitously expressed (Adapted from Blake *et al.*, 2002).